International Journal of Applied Engineering Research ISSN 0973-4562 Volume 12, Number 12 (2017) pp. 3075-3083

Iris Recognition Based on Unique Iris Templates for Reliable Personal Authentication

Shailender Kumar[1], Krishnanand Mishra[2] and Rahul Vashisht[3]

[1,2]Department of Computer Science and Engineering,
Ambedkar Institute of Advanced Communication Technologies & Research, Delhi, India.
[3]Department of Mathematics,Indian Institute of Space Science and Technology,Kerala,India.

[1]ORCID: 0000-0003-4244-2299, [2]ORCID: 0000-0002-8495-9803, [3]ORCID: 0000-0001-8414-2097

Abstract

The automatic recognition of an individual using the exclusive biometric trait like iris is the latest sensation in the field of biometric applications. The enormous mathematical advantages provided by iris pattern recognition make it hugely popular amongst the real time commercial applications which involve large scale databases. In recent years, we have witnessed several newly proposed methods attracting a lot of attention in the biometrics literature. Most of these methods basically use Daugman's algorithm with a slight variation and claim to be very promising in terms of efficiency. However, there has been barely any effort to ensure the uniqueness of iris pattern and account for the rotational inconsistencies present in the iris images while capturing them. After analyzing the recently developed frameworks, the authors of this paper have proposed an unaccustomed approach which considers these aspects which are usually neglected in the methods proposed so far. This paper gives an insight of our system designed by a novel approach and presents the performance achieved by it over two standard iris image datasets of IIT Delhi and CASIA1. Our approach outperforms the well-known existing methods over these two different datasets on the basis of experimental results obtained. Moreover, it is illustrated that we have significantly reduced both the FAR and FRR at a unique separation point which is a remarkable accolade in this field. We have almost achieved perfect recognition with FAR and FRR of 0.001% and 0.069% respectively over the IIT Delhi and CASIA1 dataset.

Keywords: automatic segmentation, face recognition,iris recognition, shape.

INTRODUCTION

Since very long time there has been a need for automatic recognition of persons. The major constraint in all of the recognition methods evolved so far has been the extent of degree up to which these methods can handle the variability between the instances of inter-class and intra-class. Reliable classification of the objects is possible only if the variability factor diverge significantly from the different elements of the same class to different classes. It can be better explained by illustrating an example like face recognition where face- a variable social organ and a three dimensional object which displays a variety of expressions presents a lot of difficulty as its image varies significantly with respect to the age, illumination, environment, pose and the viewing angle. The results show that even the best available algorithms provision an error rate of 42%-48% for the images taken at the interval of at least one year [1]. This problem enlarges itself even more in the case of inter class images as although distinct but different faces consist of near about same elementary features in the same geometrical alignment.

The above stated reasons make iris pattern as an exciting option for the secured recognition process. This approach can be reliably used when image of the iris can be captured from very near distance and in particular when there is a necessity to rummage around huge databases without any incidence of false acceptance or false rejection. The great mathematical advantage which iris provides is that in spite of being small and herculean to image, the variability in between the pattern of different persons is gigantic. The other by products of using iris as a metric for recognition is that being an internal organ it is well secluded from the environment and constant over time. Since it is a planar object its image is not so sensitive to the angle by which light is falling upon. Even if the viewing angle varies it affects the image only in form of affine transformation which is not a major concern. Another positive aspect of using iris patterns is that if somewhere pattern distortion of non-affine nature occurs then it can be readily removed and converted back to the normal state.The schematic diagram of iris recognition is represented in fig. 1.

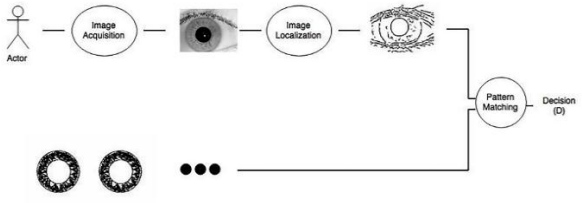

Figure 1: Schematic diagram of IRIS recognition.

The formation of iris starts approximately from the third month of gestation and the structures responsible for its unique pattern are almost developed by the eighth month. The structure and pattern of an iris is of high degree of complexity as it contains various exclusive features such as rings, corona, ridges, crypts, arching ligaments etc. Melanin pigment is the biological factor which is responsible for the colour of an iris [2,3]. Its density in the frontal layer and stroma is crucial for the colour of an iris and its absence causes the irises to be blue coloured.

The rest of this paper is organized as follows. Next section surveys the background and related work on iris recognition. Major limitations of previous work are also discussed. Section 3 describes the methodology proposed for template matching and iris recognition. Section 4 reports experiments conducted for empirical evaluation of the system and presents the results obtained. Finally, Section 5 summarizes the contributions of this paper and gives an outlook to future work.

BACKGROUND

The iris recognition using study of the iris texture has fascinated plenty of interest and researchers have offered a wide range of approaches in their respective works [1,3]. Daugman[1] has proposed extremely precise 2-D Gabor filter based technique for the iris recognition system that engaged 2048 bit iris-code. He has also given the most exciting empirical results obtained from the private databases being used at large scale. Boles [4] has provided fine-to-coarse ballpark figure at distinct levels of resolution which are based on zero-crossing expression from the wavelet conversion decomposition. Wildes et al. [2, 5] have emphasized on proficient realization of iris segmentation which are based on gradient oriented Laplacian pyramid. Proenca and Alexandre [6] have recommended that for the iris images captured from the large distances region-based feature extraction should be applied. Recently non-linear contortions from the iris designs have been predicted by the Thornton et al. [7] who have also suggested a Bayesian approach for dependable performance advancement. An another approach which outperformed the prior used techniques was proposed by Huang et al. [8] who established the practice of phase-based local co- relations for verifying the iris patterns for similarity. In a research paper authored by Ma et al. [9, 10] comparison of multi scale band pass decomposition with the prior approaches on the basis of performance is presented .They also proposed a valuable substitute for iris detection using Gaussian–Hermite moments yanked from the intensity signals of iris in one dimension [10]. In [1] the authors have detailed the condensed depiction of iris attributes by means of moment invariants extracted from the Gabor wavelet features and have stated that their approach tenders promising results. Sanchez-Avila et al. have made exciting modification in the technique suggested in [11]. Exact localization of iris and eyelash area is the solution to the efficient iris recognition and has been the center of research in [12, 13]. Yu et al. [14] seem to be influenced by the technique applied in fingerprint recognition and have tried to employ the similar process for iris recognition by extracting the key points from iris templates.

METHODOLOGY

Our approach consists of five main steps which have been shown in the fig. 2. They are as: (a) Iris Localization (b) Iris Segmentation (c) Iris Normalization (d) Feature Encoding (e) Template Matching.

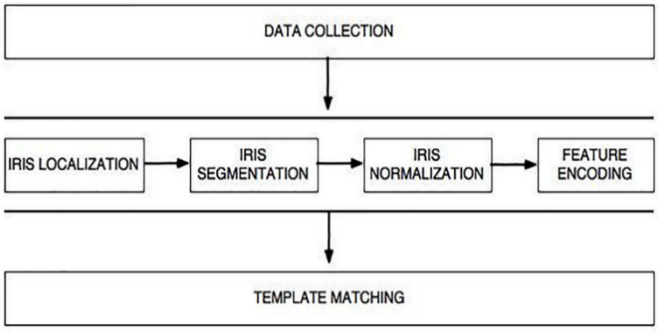

Figure 2: Illustrates the flow diagram of steps involved.

Iris Localization

It can't be assumed that the boundaries of iris and pupil are strictly concentric in nature in spite of the fact that results obtained after the iris search put a huge constraint on the pupil search. More often than not the iris centre is superior and nasal with respect to the pupil center. The range of the pupil radius lies in between the 0.1 to 0.7 of the iris radius. It is precautionary to estimate the parameters which define the pupillary circle in separation to those which define the iris. These parameters can be determined by using an integral differential parameter which is represented as:

$$\max\left(r, x_0, y_0\right) G_\sigma(r) * \frac{\partial}{\partial r} \oint_{r,x_0,y_0} \frac{I(x,y)}{2\pi r} ds \quad (1)$$

Where, I (x,y) = an image lying in the image domain.

r = increasing radius

ds=circular arc of radius r

(x_0, y_0) = central coordinates

The Daugman's [15, 16] system fits the circular contours via gradient ascent on the parameters so as to maximize:

$$\frac{\partial}{\partial r} G(r) * \oint_{r,x_c,y_c} \frac{I(x,y)}{2\pi r} ds \quad (2)$$

Where G(r)is a radial Gaussian, and circular contours (for the limbic and pupillary boundaries) to be parameterized by

center location(x_c, y_c) and radius r (active contour fitting method).

Our system performs its contour fitting in two steps:

First, the image intensity information is converted into a binary edge-map:

$$|\nabla G(x, y) * I(x, y)| \quad (3)$$

Where,

$$G(x, y) = \frac{1}{2\pi\sigma^2} e^{-\frac{(x-x_0)^2+(y-y_0)^2}{2\sigma^2}} \quad (4)$$

And,

$$\nabla \equiv \left(\frac{\partial}{\partial x}, \frac{\partial}{\partial y}\right) \quad (5)$$

Equation 4 and equation 5 mathematically explicate this step.

Second, the edge points vote to instantiate particular contour parameter values and the voting procedure of our system is realized via Hough transforms on parametric definitions of the iris boundary contours. This step is mathematically explained by equation 6.

$$H(x_c, y_c, r) = \sum_{j=1}^{n} h(x_j, y_j, x_c, y_c, r) \quad (6)$$

Where,

$$h\left(x_j, y_j, x_c, y_c, r\right) = \begin{cases} 1, & \text{if } g\left(x_j, y_j, x_c, y_c, r\right) = 0 \\ 0, & \text{otherwise} \end{cases} \quad (7)$$

$$g\left(x_j, y_j, x_c, y_c, r\right) = (x_j - x_c)^2 + (y_j - y_c)^2 - r^2 \quad (8)$$

The presence of operator in equation 1 serves the purpose of finding the two boundaries named as pupillary boundary and outer boundary of irises. The signs of the existence of an interior pupil are found while performing the primary search for the limbus which is very encouraging as limbic boundary helps largely in improving the robustness. They turn out to be very effective in providing the robust nature since usually against the long wavelength NIR illumination they have highly soft contrast. We follow the similar approach as described by the Daugman in [1, 16] for detecting the curvilinear edges which in effect localizes both the upper and lower boundaries of eyelids. We achieved our target of reaching the highest precision level for both these boundaries which may scrutinize even the single pixel. We changed the course of outline integration from spherical to arcuate, and applied spline parameters for modeling the boundary of eyelids after performing statistical analysis. Those Images in which the visibility of the iris present between the fitted eyelid splines is less than the 60% are considered as inappropriate for the recognition [17].

Segmentation

When the iris localization is over our next step is to segregate the actual iris area from the captured image of eye. This stage is called as iris segmentation. Two circles which are almost concentric approximate the iris region. The exterior one covers the iris/sclera boundary while the interior one covers the iris/pupil boundary. Occlusion of the higher and lower parts of the iris region is done by the eyelids and eyelashes respectively. Specular reflections are a major hindrance in this process as they corrupt the regular pattern of the iris. We used the Hough transform technique for locating the circular iris area along with separating and eliminating the artifacts like specular reflections. Our approach is largely dependent on the quality of the captured image [18]. The segmentation process becomes pretty difficult for the irises which have pretty dark pigments as there is very low contrast between the pupil and iris region in these cases [19, 20]. It is advisable that such iris images should not be captured under the natural light as our segmentation process is highly affected by the illumination. This stage is very significant to our approach as biometric templates may be corrupted by the malign data veiled in the form of an iris pattern and that will affect the recognition rates very adversely.

Hough transform

The most widely used algorithm for determining the geometrical parameters of an image such as lines and circles is Hough transform. We applied circular Hough transform to extrapolate the required coordinates of center and radius of the pupil and iris area. It's an automatic segmentation algorithm. It produces the edge map by computing the first derivatives of intensity values and then thresholds the obtained results. It detects the parameter of circle crossing through each edge point from the refined edge map in Hough space. The parameters are $(x_c, y_c)$and r which are the coordinates of centre and radius respectively. They correspond to the maximum point in the Hough space. They describe the locus of circle as per the equation 9.

$$x_c^2 + y_c^2 - r^2 = 0 \quad (9)$$

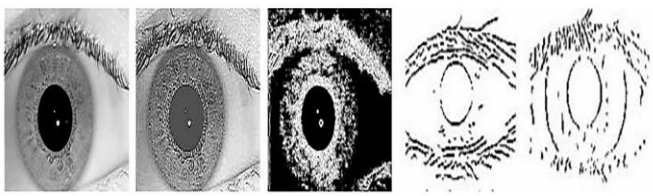

Figure 3: A sample eye image (IIT Delhi database) and its horizontal and vertical edge map.

We also used parabolic Hough transform for detecting the eyelids and representing them through parabolic arcs described by the equation 10.

$$(-(x - h_j)\sin\theta_j + (y - k_j)\cos\theta_j)^2 = aj((x - h_j)\cos\theta_j + (y - k_j)\sin\theta_j) \quad (10)$$

Where,

$aj -$ Controls the curvature

$(h_j, k_j) -$ Peak of the parabola

$\theta_j -$ Angle of rotation relative to the x-axis.

In circular Hough transform the horizontal direction derivatives are for identifying the upper and lower eyelids while the vertical one is for identifying the exterior boundary line of the iris as shown in fig.3. The impetus for this comes from the fact that generally eyelids lie in horizontal alignment only and hence using all the gradient data for eyelid edge map may disrupt the continuity of circular iris boundary edge map [1, 21]. In our approach we have applied circular Hough transform where only the vertical gradients are considered for identifying the iris boundary and not all the circle defining edge pixels. This reduces the underlying influence of both the upper and lower eyelids. Moreover, it makes the circle localization more effective and elegant as the number of edge points which contributes in the Hough space reduces significantly.

Normalization

When the iris section is profitably segmented from an eye image, our next goal is to convert the iris area so that constant dimensions are available for the comparison purpose. Varying levels of lighting causes pupil dilation which is the primary source of the dimensional inconsistency. Inconsistency also arises from several other sources like rotation of the eye within the eye socket, rotary motion of the camera, unstable imaging and head tilt. The major function of the normalization procedure is to generate such iris regions, which can be termed as alike from the dimensional point of view so that two different images of the same iris captured under diverse conditions will have the same attributes at the same spatial position [22]. It is not necessary that both the pupil region and iris region always have the co-center and usually the location of pupil region is nearly nasal. We have accounted for this factor so as to get the constant radius even for the iris regions which have shape of a ring.

Feature Encoding

Every iris pattern contain a lot of information but not all of them are required for the recognition purpose .The most essential features which contain the distinct information about an iris pattern are encoded only [15, 23]. We used the band pass decomposition for creating the iris template and applied a logical metric for comparing two iris templates. The range of values of the degree of similarity for the iris templates of same eye is different than those for the templates belonging to the different eyes. It helps in getting a clear idea that whether two iris templates belong to the same eye or different by providing exclusive values for these two cases.

Pattern Matching

Once we have accomplished the task of localization over the captured image, then our next and final goal is to confirm that whether the pattern under consideration matches with any of the earlier warehoused patterns. The pattern matching process can be completely described in the following steps and these steps are accomplished by applying below stated standard equations for pattern matching. The first two steps are mathematically explained by equation 11 and equation 12 while the remaining two steps are mathematically explicated by equation 12 and equation 13.

1) To bring the freshly captured iris template into 3-D alignment.

2) To select a representative of aligned iris patterns that makes their unique patterns evident in nature.

3) To assess the degree of match between the freshly captured pattern and formerly stored patterns.

4) To confirm that whether the freshly arrived entry and the already established entry in the database are extracted from the same iris.

$$h_{Re} = 1 \quad \text{if Re} \int_\rho \int_\varphi e^{-i\omega(\theta_0-\varphi)} e^{-\frac{(r_0-\rho)^2}{\alpha^2}} e^{\frac{-(\theta_0-\varphi)^2}{\beta^2}} I(\rho,\varphi)\rho d\rho d\varphi \geq 0 \quad (11)$$

$$h_{Re} = 0 \quad \text{if Re} \int_\rho \int_\varphi e^{-i\omega(\theta_0-\varphi)} e^{-\frac{(r_0-\rho)^2}{\alpha^2}} e^{\frac{-(\theta_0-\varphi)^2}{\beta^2}} I(\rho,\varphi)\rho d\rho d\varphi < 0 \quad (12)$$

$$h_{Im} = 1 \quad \text{if Im} \int_\rho \int_\varphi e^{-i\omega(\theta_0-\varphi)} e^{-\frac{(r_0-\rho)^2}{\alpha^2}} e^{\frac{-(\theta_0-\varphi)^2}{\beta^2}} I(\rho,\varphi)\rho d\rho d\varphi \geq 0 \quad (13)$$

$$h_{Im} = 0 \quad \text{if Im} \int_\rho \int_\varphi e^{-i\omega(\theta_0-\varphi)} e^{-\frac{(r_0-\rho)^2}{\alpha^2}} e^{\frac{-(\theta_0-\varphi)^2}{\beta^2}} I(\rho,\varphi)\rho d\rho d\varphi < 0 \quad (14)$$

In our system we have applied Hamming distance as metric for the matching of iris templates. Only those bits which are produced from the real iris area are considered for calculating

the hamming distance. This approach provides our system an edge over the others as it encompasses noise masking [16, 24]. It means that only those significant bits that correspond to '0' bit in noise masks of both the templates are used for calculating the hamming distance.

The formula for evaluating this modified hamming distance in our system is given by equation 15.

$$\text{Hamming Distance} = \frac{1}{N-\sum_{k-1}^{N} Xn_k(OR)Yn_k} \sum_{j-1}^{N} X_j(XOR)Y_j(AND)Xn'_j(AND)Yn'_j \quad (15)$$

Where,

X_j and Y_j = Bit wise templates required for comparison.

Xn_j and Yn_j = Noise masks corresponding to X_j and Y_j respectively.

N = number of bits each template represent.

Theoretically the hamming distance value for the two iris templates of same eye should be 0.0 but practically it is not possible. It happens due to the factors like imperfect normalisation and undetected noises.

Shifting process

Although we take proper care to maintain the uniqueness of an iris pattern but still there remains rotational inconsistency which has to be removed. For this purpose we performed shifting where a template is shifted one bit towards left and then one bit towards right before calculating its hamming distance with other template. An example of shifting is illustrated in fig.4. This is called as horizontal shifting in which angular resolution (θ) decides the angle by which actual iris region is rotated [25, 26]. In our system the value of is 180^0 which means that for each shift in the bit, the iris template rotates by two degrees. The maximum difference between the angles of two iris images belonging to the same eye decides the exact number of shifts required for removing the rotational inconsistency. This method ensures that the irregularities in the normalised iris pattern rooted from the rotational differences while capturing the image is rectified.

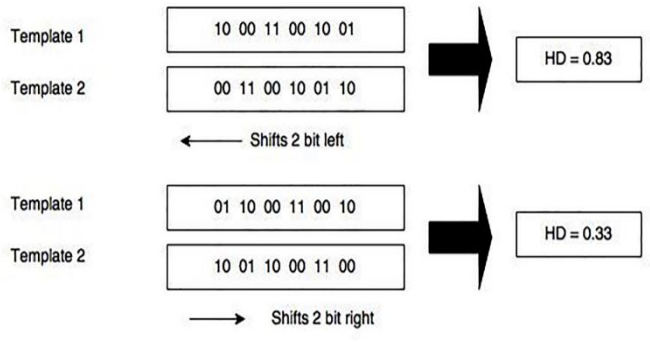

Figure 4: An illustration of the shifting process.

EMPIRICAL EVALUATION AND RESULTS

Dataset And Software

We have used the dataset of IIT Delhi [27] and it consists of 2550 color eye images taken using a C.C.D. Camera. The details about the datasets used and comparisons made are represented in Table 1. Since the images were captured using natural light, specular reflections are present on the pupil regions. This database is also captured for iris recognition purpose. Our proposed automated approach was implemented and tested in MATLAB.

Table 1: Datasets used for testing the system.

Dataset Name	Number of eye images	Intra-class Comparisons	Inter-class Comparisons
IIT-DELHI	224	1248	24,382
CASIA 1	108	367	4046

Experimental Settings

In this subsection we shall describe about the performance of our iris recognition system and the necessary internal details required for achieving that kind of performance. We conducted several tests to figure out the exact point at which we get the best separation. From the term 'best separation' used here we mean that there is a clear distinction between the inter-class pattern matching and intra-class pattern matching. It was required for reducing the false acceptance rate and false rejection rate as much as possible so that our system works accurately for the recognition purpose. When there is a clear separation hamming distance value available, then a decision can be made with high confidence regarding inter-class comparisons and intra-class comparisons [1,3]. If the hamming distance generated while comparing the two iris templates is less than or equal to the separation value, then templates are assumed to be produced from the same iris otherwise they are considered to be belonging from different irises. The parameters required for iris recognition are radial and angular resolution represented by r and θ respectively. We considered optimum values of both these parameters for efficient recognition. In order to overcome the rotational inconsistency we also considered the shifting process as explained under the pattern matching section.

Uniqueness of the iris patterns

In order to be sure about the uniqueness of a given iris pattern we reduced the degree of freedom (DOF) in its template representation and then conducted tests to confirm the uniqueness. It was required in our system as the success of recognition depends entirely upon the fact that two iris

patterns of different eyes should be completely exclusive in every aspect. While testing the statistical independence of two irises if there is a failure then it means that both belong to same eye and final output comes as 'matched' [15, 19].

We determined the uniqueness of an iris pattern through inter class comparisons and analyzed the admeasurements of hamming distance values generated. Going by the statistical theory the mean of hamming distance for the interclass comparisons should be 0.5. We can say this because if the bits are completely independent, then half of the chance is that it is set as '0' and rest of the half is that it is set as'1'. As a result, on an average about half of the number of bits matches between the two iris templates and hence hamming distance should come as 0.5. Since we also accounted for the rotational inconsistency by shifting the templates from left to right, our mean hamming distance for the interclass comparison came out to be little less than 0.5. It happened because the lowest hamming distance value out of the various others produced during comparisons was considered for each of the shifted template. In our system the mean hamming distance is inversely proportional to the number of shifts applied for removing the rotational inconsistency.

Decidability

It is a metric which is used to find out the separation between inter-class and intra-class comparisons. It depends upon the mean and standard deviation of the hamming distance of the hamming distance values distributed binomially over a range for the inter class and intra class comparisons [16, 21]. The standard formula for calculating the decidability is given by equation 16.

$$d' = \frac{|\mu_S - \mu_D|}{\sqrt{(\frac{\sigma_S{}^2}{2} + \frac{\sigma_D{}^2}{2})}} \quad (16)$$

Where,

$d' =$ decidability

$\mu_s =$ mean of the intra $-$ class distribution

$\mu_D =$ mean of the inter $-$ classdistribution

$\sigma_s{}^2 =$ standard deviation of the intra $-$ class distribution

$\sigma_D{}^2 =$ standard deviation of the inter $-$ class distribution

Table 2 and Table 3 reflect the decidability values for IIT Delhi and CASIA1 dataset respectively.

Table 2: Decidability values of the IIT Delhi dataset.

Filter bandwidth (σ/f)	Intra class distribution mean (μ_s)	Inter class distribution mean (μ_D)	Intra class distribution standard deviation ($\sigma_s{}^2$)	Inter class distribution standard deviation ($\sigma_D{}^2$)	Decidability (d')
0.5	0.24	0.47	0.003769	0.000590	5.08
0.5	0.25	0.47	0.004369	0.001513	4.01
0.7	0.25	0.47	0.004083	0.000566	4.72
0.7	0.25	0.47	0.004225	0.001274	4.16
0.5	0.23	0.48	0.003721	0.000331	5.34
0.5	0.24	0.48	0.003648	0.000278	5.38
0.7	0.25	0.47	0.003881	0.000924	4.55
0.7	0.24	0.48	0.003918	0.000302	5.07
0.5	0.26	0.46	0.006115	0.004610	2.78

Table 3: Decidability values of the CASIA 1 dataset.

Filter bandwidth (σ/f)	Intra class distribution mean (μ_s)	Inter class distribution mean (μ_D)	Intra class distribution standard deviation ($\sigma_s{}^2$)	Inter class distribution standard deviation ($\sigma_D{}^2$)	Decidability (d')
0.5	0.26	0.44	0.001953	0.001030	4.54
0.3	0.28	0.45	0.001528	0.000475	5.27
0.5	0.27	0.45	0.001713	0.000501	5.50

The higher values of decidability provides higher accuracy in terms of recognition since the separation between the inter class distributions and intra class distributions becomes larger which means that there is a little window for overlapping region. It also prevents the outlier values to corrupt the recognition process as they are straightaway rejected. However there is still some overlap between the inter class distributions and intra class distributions which is demonstrated in the following fig. 5.

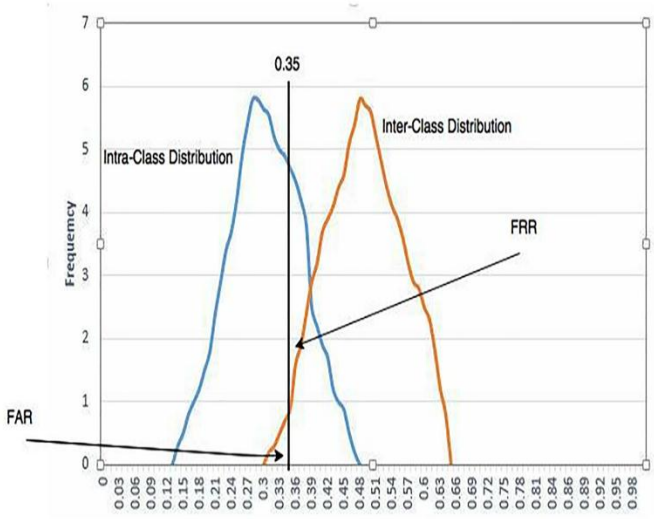

Figure 5: Intra class and Inter class Hamming Distance distribution with overlap.

This overlapping region corresponds to the false acceptance and false rejection phenomenon which occurs while recognition. False acceptance rate (FAR) is the probability of an imposter being identified as authentic while recognition. It is calculated by using equation 17.

$$\mathrm{FAR} = \frac{\int_0^k P_{DIFF}(x)dx}{\int_0^1 P_{DIFF}(x)dx} \quad (17)$$

Where,

$P_{DIFF} -$ inter class distribution

$k -$ separation point

False rejection rate (FRR) is the probability of an authentic person being identified as imposter and hence denied access to the system. It is calculated by using equation 18.

$$\mathrm{FRR} = \frac{\int_k^1 P_{same}(x)dx}{\int_0^1 P_{same}(x)dx} \quad (18)$$

Where,

$P_{same} -$ intra class distribution

$k -$ separation point

In the following section the performance of our iris recognition system as recorded after examining and verifying the system as a whole over the standard datasets is being represented in the form of results.

Results

Table 4 shows the FAR and FRR of our system obtained at different threshold values over the IIT Delhi dataset. Table 5 shows the FAR and FRR of our system obtained at different threshold values over the CASIA1 dataset [28].

Table 4: FAR and FRR for the IIT-DELHI dataset at different thresholds.

Threshold	FAR (%)	FRR (%)
0.20	0.000	76.046
0.25	0.000	43.802
0.30	0.000	22.191
0.35	0.000	0.001
0.40	0.000	2.414
0.45	2.213	0.000
0.50	90.147	0.000

Table 5: FAR and FRR for the CASIA dataset at different thresholds.

Threshold	FAR (%)	FRR (%)
0.20	0.000	99.162
0.25	0.000	80.009
0.30	0.000	36.640
0.35	0.000	0.138
0.40	0.005	1.192
0.45	7.599	0.000
0.50	99.499	0.000

Fig. 6 represents the accuracy of our system in terms of FAR and FRR for both the authentic and imposter match at different thresholds as obtained while testing the system for both datasets.

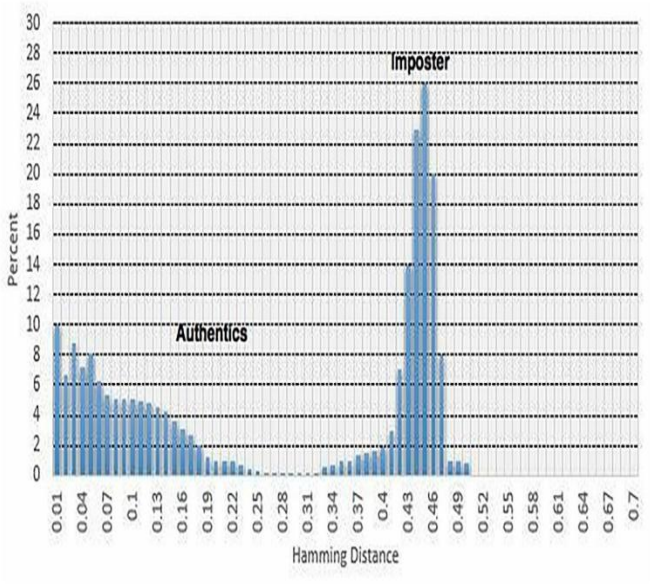

Figure 6: Verification distribution of authentic and imposter recognition.

CONCLUSION AND FUTURE WORK

The system designed with this novel approach outperforms the renowned existing methods over these two standard datasets. For the IIT Delhi dataset we have achieved perfect recognition by selecting the threshold as 0.35 which gives false accept rate and false reject rate both as 0.00%. For the CASIA1 dataset perfect recognition is not possible but we have achieved highly appreciable FAR and FRR of 0.000% and 0.138% respectively at the same threshold of 0.35 and it allows for accurate recognition It is remarkable that we have successfully reduced both the FAR and FRR up to such large extent at a unique separation point for these two datasets.

It would turn out to be beneficial if we incorporate some eminence measures for the enrolled images as in effect it enhances the reliability of the iris recognition system. It would then permit us the leverage to evaluate the quality of each gathered image so that it must be of minimum acceptable level for feature matching. Our approach turned out to be robust in nature during our experimental study as it produced satisfactory results even for the interlaced or blurred images. However, it can get influenced by other factors like severe blurring, high dilation and off angle iris. Moreover heavy occlusion and bad illumination would affect our approach severely if compared with the traditional approach. When colossal occlusions are present then they may extensively lessen the number of visual features which can be applied for the pattern matching. The contrast quality shall be very poor in the case of poor illumination which may result in detection of fewer features.

REFERENCES

[1] Daugman, J. "How iris recognition works. Proceedings of 2002 International Conference on Image Processing.", 2002.

[2] Wildes, Richard P. "Iris recognition: an emerging biometric technology." Proceedings of the IEEE 85, no. 9,pp. 1348-1363. 1997.

[3] Chen, Jianxu, Feng Shen, Danny Ziyi Chen, and Patrick J. Flynn. "Iris recognition based on human-interpretable features." IEEE Transactions on Information Forensics and Security 11, no. 7, pp. 1476-1485, 2016.

[4] Boles, Wageeh W., and BoualemBoashash. "A human identification technique using images of the iris and wavelet transform." IEEE transactions on signal processing 46, no. 4, pp. 1185-1188, 1998.

[5] Wildes, Richard P., Jane C. Asmuth, Gilbert L. Green, Stephen C. Hsu, Raymond J. Kolczynski, James R. Matey, and Sterling E. McBride. "A system for automated iris recognition." In Applications of Computer Vision, 1994., Proceedings of the Second IEEE Workshop on, pp. 121-128. IEEE, 1994.

[6] Proenca, Hugo, and Luis A. Alexandre. "Toward noncooperative iris recognition: A classification approach using multiple signatures." IEEE Transactions on Pattern Analysis and Machine Intelligence 29, no. 4, 2007.

[7] Thornton, Jason, MariosSavvides, and BVK Vijaya Kumar. "A Bayesian approach to deformed pattern matching of iris images." IEEE Transactions on Pattern Analysis and Machine Intelligence 29, no. 4, 2007.

[8] Huang, Jun-Zhou, Tie-Niu Tan, Li Ma, and Yun-Hong Wang. "Phase correlation based iris image registration model." Journal of Computer Science and Technology 20, no. 3 pp. 419-425, 2005.

[9] Ma, Li, Yunhong Wang, and Tieniu Tan. "Iris recognition using circular symmetric filters." In Pattern Recognition, 2002. Proceedings. 16th International Conference on, vol. 2, pp. 414-417. IEEE, 2002.

[10] Ma, Li, Tieniu Tan, Yunhong Wang, and Dexin Zhang. "Efficient iris recognition by characterizing key local variations." IEEE Transactions on image processing 13, no. 6, pp. 739-750, 2004.

[11] Sanchez-Avila, Carmen, and Raul Sanchez-Reillo. "Two different approaches for iris recognition using Gabor filters and multiscale zero-crossing representation." Pattern Recognition 38, no. 2, pp. 231-240, 2005.

[12] Kong, Wai-Kin, and David Zhang. "Detecting eyelash and reflection for accurate iris segmentation." International journal of pattern recognition and artificial intelligence 17, no. 06, pp. 1025-1034, 2003.

[13] Kong, W. K., and D. Zhang. "Accurate iris

segmentation based on novel reflection and eyelash detection model." In Intelligent Multimedia, Video and Speech Processing, 2001. Proceedings of 2001 International Symposium on, pp. 263-266. IEEE, 2001.

[14] Yu, Li, David Zhang, and Kuanquan Wang. "The relative distance of key point based iris recognition." Pattern Recognition 40, no. 2, pp. 423-430, 2007.

[15] Daugman, John G. "High confidence visual recognition of persons by a test of statistical independence." IEEE transactions on pattern analysis and machine intelligence 15, no. 11, pp. 1148-1161, 1993.

[16] Daugman, John. "Probing the uniqueness and randomness of IrisCodes: Results from 200 billion iris pair comparisons." Proceedings of the IEEE 94, no. 11, pp. 1927-1935, 2006.

[17] Lim, Shinyoung, Kwanyong Lee, OkhwanByeon, and Taiyun Kim. "Efficient iris recognition through improvement of feature vector and classifier." ETRI journal 23, no. 2, pp. 61-70, 2001.

[18] Kumar, Ajay, and ArunPassi. "Comparison and combination of iris matchers for reliable personal authentication." Pattern recognition 43, no. 3, pp. 1016-1026, 2010.

[19] He, Xiaofu, and Pengfei Shi. "A new segmentation approach for iris recognition based on hand-held capture device." Pattern Recognition 40, no. 4, pp. 1326-1333, 2007.

[20] Sanderson, S., and J. H. Erbetta. "Authentication for secure environments based on iris scanning technology." IEE Colloquium on Visual Biometrics, 2000.

[21] Daugman, John G. "Biometric personal identification system based on iris analysis." U.S. Patent 5,291,560, issued March 1, 1994.

[22] Nohl, Seung—In, KwanghukPael, ChulhanLeel, and Jaihie Kim. "Multiresolution Independent Component Analysis for Iris Identification." The 2002 International Technical Conference on Circuits/Systems, Computers and Communications, Phuket, Thailand, 2002.

[23] Zhu, Yong, Tieniu Tan, and Yunhong Wang. "Biometric personal identification based on iris patterns." In Pattern Recognition, 2000. Proceedings. 15th International Conference on, vol. 2, pp. 801-804. IEEE, 2000.

[24] Tisse, Christel-loic, Lionel Martin, Lionel Torres, and Michel Robert. "Person identification technique using human iris recognition." In Proc. Vision Interface, pp. 294-299. 2002.

[25] Ritter, Nicola, Robyn Owens, J. Cooper, and Paul P. Van Saarloos. "Location of the pupil-iris border in slit-lamp images of the cornea." In Image Analysis and Processing, 1999. Proceedings. International Conference on, pp. 740-745. IEEE, 1999.

[26] Burt, Peter, and Edward Adelson. "The Laplacian pyramid as a compact image code." IEEE Transactions on communications 31, no. 4, pp. 532-540, 1983.

[27] IITDIrisDatabase, <http://web.iitd.ac.in/_biometrics/Database_Iris.htm>, 2008.

[28] CASIAIRISDatabase, <http://www.cbsr.ia.ac.cn/english/IrisDatabase.asp>, 2008.